A data-driven two-lane traffic flow model based on cellular automata

Peer-reviewed author version

Shang , Xue-Cheng; Li, Xin-Gang; Xie, Dong-Fan; Jia , Bin; Jiang , Rui & LIU, Feng (2022) A data-driven two-lane traffic flow model based on cellular automata. In: Physica. A (Print), 588 (Art N° 126531).

DOI: 10.1016/j.physa.2021.126531
Handle: http://hdl.handle.net/1942/36494

A data-driven two-lane traffic flow model based on cellular automata

Xue-Cheng Shang[a], Xin-Gang Li[a], Dong-Fan Xie[a], Bin Jia[a], Rui Jiang[a], Feng Liu[b]

[a] Key Laboratory of Transport Industry of Big Data Application Technologies for Comprehensive Transport, Beijing Jiaotong University, Beijing 100044, China

[b] Transportation Research Institute (IMOB), Hasselt University, Wetenschapspark 5, bus 6, B-3590 Diepenbeek, Belgium

Abstract

In this paper, a data-driven two-lane traffic flow model based on cellular automata is proposed. Long Short-Term Memory (LSTM) and Support Vector Machine (SVM) are used to learn the characteristics of car following behavior and lane changing behavior, respectively, from real operation data of vehicles. Under optimal network parameters, the mean absolute errors of the LSTM network for training and testing data are only 0.001 and 0.006, respectively; while the prediction accuracy of the SVM classifier for both data reaches higher than 0.99. Moreover, forward rules and lane changing rules which are more consistent with actual situation are designed. The simulation results of the proposed model show that: (1) the new model can reflect the first-order phase transition from free flow to synchronized flow; (2) the frequency of unsuccessful lane changing is near zero in low-density traffic areas, but increases sharply in high-density regions; and (3) the lane changing duration and unsuccessful lane changing frequency display similar trends as traffic densities increase.

Key words: cellular automata; lane changing; Long Short-Term Memory; Support Vector Machine; data-driven

1. Introduction

In recent years, traffic problems (such as traffic jam, environmental pollution, etc.) have become increasingly serious. In order to solve these problems, scholars and researchers have developed various traffic flow models, ranging from continuous [1, 2] and gas-kinetic-based [3-5] to car following [6, 7] and cellular automata [8] models. In addition, neural networks and machine learning, especially deep learning technology (such as Long Short-Term Memory (LSTM) [10-12] and Support Vector Machine (SVM) [9]) have been widely adopted to extract the characteristics of driving behavior and the inherent evolution mechanism of traffic flow [9-22].

Among the existing traffic flow models, cellular automata (CA) has been a major technique because of the flexibility and transparency of the modelling process [23], based on which certain characteristics of traffic flow can be well simulated [24-43]. CA includes the famous Nagel-Schreckenberg (NaSch) model as well as a number of improved models, such as the BJH, VDR, TT, safety driving model, brake light model, KKW, LAI, etc. In addition to transport networks, CA has also been utilized for the analysis of a variety of other systems [23, 44-60]

Car following and lane changing are the most important behavior in driving. Traditional CA models can simulate some macroscopic phenomena of car following behavior, but they cannot describe the details of lane changing processes well. The updating rules of the models [61] on acceleration, deceleration and random slowing down are not consistent with the reality. According to the models, the vehicle will change to the target lane immediately after satisfying lane changing rules. However,

in practice, lane changing is a process involving several steps; it is impossible for the driver to complete these operations at the same time (i.e. in one time step). In order to describe lane changing processes more reasonably, we proposed the TCA-H model based on CA in the previous study [62]. In this model, a rough algorithm for calculating lane changing duration according to actual situation was introduced. Nevertheless, driving behavior is a complex phenomenon, affected not only by surrounding traffic conditions but also by personal driving habits. Therefore, a more appropriate method than the rough algorithm [62] to mine drivers' driving behavior should be considered.

Deep learning technology has shown good capacity in data mining as well as in portability, and in recent years has been applied to study car following behavior and lane changing behavior (including lane changing decision and lane changing trajectories) [10, 12]. However, few studies have focused on unsuccessful lane changing behavior.

In order to better characterize driving behavior particularly unsuccessful lane changing behavior, we propose a new model in this paper. The main contributions of this study include: (1) building a data-driven two-lane traffic flow model based on cellular automata; (2) improving the problem of constant and excessive acceleration of traditional CA models; (3) designing more convincing rules of unsuccessful lane changing.

The rest of this paper is organized as follows. The proposed model is described in Section 2, and further evaluated in Section 3. Finally, major conclusions are drawn in Section 4.

2. Model

In the traditional rule-based two-lane cellular automata (R-TCA) model [63] (see Fig 1.), the cell size is normally very large, leading to unrealistic acceleration and simulation of the lane changing process. Although refining cell sizes can solve the abrupt acceleration behavior, it will increase simulation time. Moreover, the updating rules of the model (on accelerating, decelerating and randomly slowing down) in the same time step are not consistent with real behavior. In order to solve these problems, we introduce a new model that is more in line with the lane changing process under actual traffic situation.

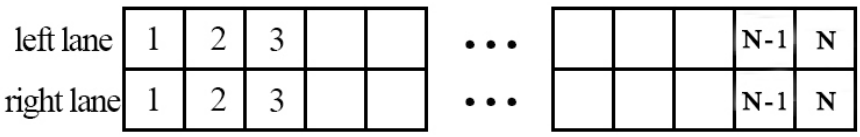

Fig.1 Cell in the R-TCA model

2.1. Discretization

The new model, namely a data-driven two-lane traffic flow (D-TCA) model, accommodates two important improvements. On the one hand, in order to better characterize the lane changing process, the cell is refined to a smaller size; on the other hand, the updating rules of the model are based on the prediction results of neural networks. In the model, the acceleration is computed based on a process more consistent with actual situation, and the longitudinal length of the cell determines the minimum acceleration of vehicles.

As shown in Fig. 2(a), the width of each lane is 3.5m, and the total width of the two lanes is 7m. Without losing generality, we use rectangular cells and choose a

certain cell size to explain the lane changing process. Set the lateral and longitudinal length of each cell to 0.25m and 0.1m, respectively (see Fig. 2(b)), leading to the width of each lane consisting of 14 cells. Assume that the length and width of the vehicle is 5m and 2m (occupying 50 and 8 cells), respectively, and that the vehicle is in the middle of the lane.

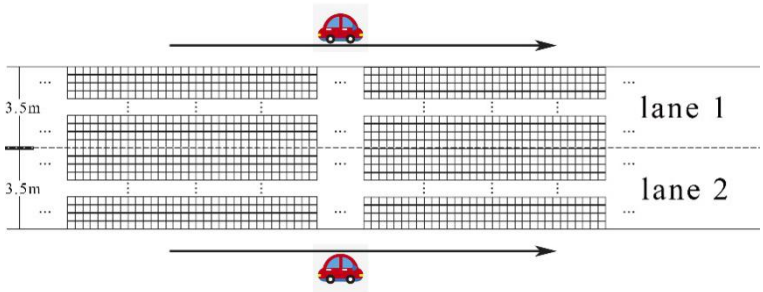

(a)

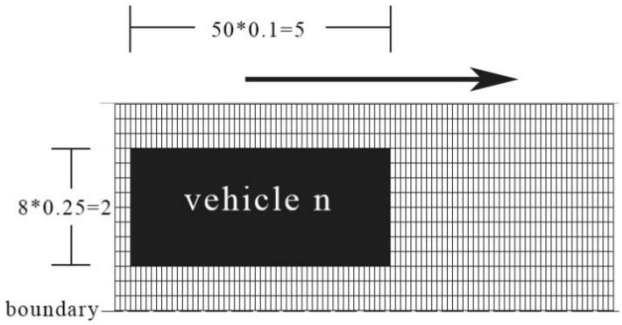

(b)

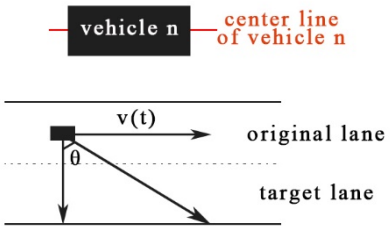

(c)

Fig.2 Cell discretization in the D-TCA model

The lane changing process of the vehicle is described as the movement along both longitudinal and lateral directions. In R-TCA, the vehicle changes lanes instantaneously; while in D-TCA, the vehicle needs several time steps to complete the lane changing maneuver. Assume of 5 different cell occupation states in the latter model, and the vehicle passes through one of these states at each time step when changing lanes. These states include:

State 0, the traffic condition of the vehicle satisfies the lane changing rules;

State 1, the vehicle leaves the center of the lane, but it does not occupy the boundary (the dividing line between the two lanes);

State 2, the vehicle occupies the boundary;

State 3, the vehicle leaves the original lane, and it does not occupy the boundary;

State 4, the vehicle reaches the center of the target lane.

To determine the state of the vehicle during lane changing, the lateral position of the vehicle is considerd. Define as the angle between the center line of the vehicle

and the lateral direction of the road (see Fig.2(c)). Given that in D-TCA (like in any other CA models), the analyzed system is regarded as a highly discrete process over both time and space, the lateral movement distance increases discretely as the time step grows. Assume that the vehicle starts the lane changing maneuver at time step k_s, the lateral distance *d(k)* of the vehicle (relative to the original lane) at time step *k* () can be calculated by Eq.(1) [62]

(1)

Where denotes the speed of the vehicle along the longitudinal direction of the road at time step *i*, and is the length of each time step. In total 192 lane changing trajectories were extracted from the experimental dataset (described in Section 2.3), and the average lane changing angle =86.78°. Thus, we take as the lane changing angle of each vehicle.

Based on *d(k)*, the state of the vehicle is decided as follows:

, the vehicle is in State 0;

, the vehicle is in State 1;

, the vehicle is in State 2;

, the vehicle is in State 3;

, the vehicle is in State 4.

2.2. Notations

, the subject vehicle ;

, the closest vehicle in front of on the original lane (the lane where originally drives);

, the cloest vehicle behind on the original lane;

, the closest vehicle in front of on the target lane (the lane to which is intended to change);

, the closest vehicle behind on the target lane;

, the acceleration of;

, the position of ;

, the velocity of ;

, the acceleration of ;

, the velocity of;

, the velocity of ;

, the velocity of ;

, the velocity of ;

, the space headway between and;

, the space headway between and;

, the space headway between and;

, the space headway between and;

, the predicted acceleration of based on the current input;

and , the maximum speed and acceleration capacity of vehicles.

Moreover, based on the previous notations, the following variables are defined.

;

;

;

.

The illustrations of some notations above can be found in Fig. 3.

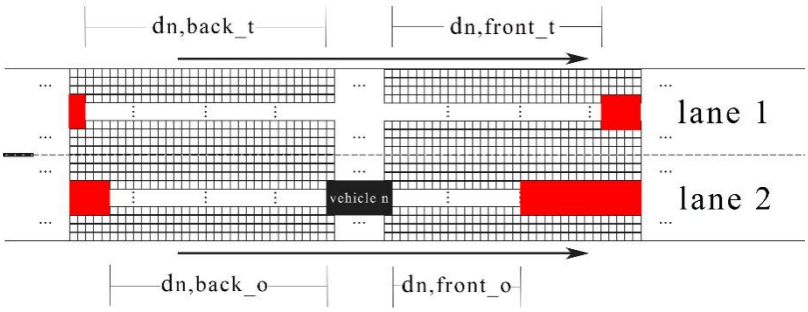

Fig. 3 The illustrations of some notations.

Note: the black rectangle, left and right red rectangles on lane 2, and the left and right red rectangles on lane 1 represent ,,,, and , respectively.

2.3. Model details

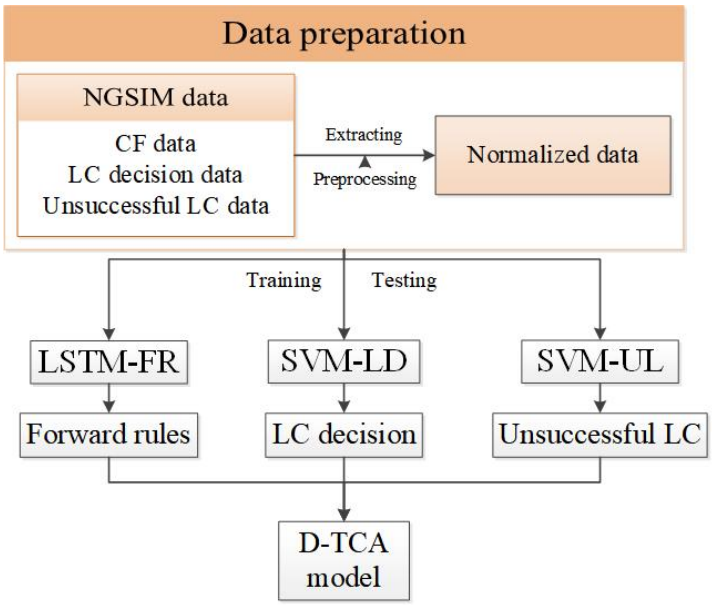

Fig.4 Framework of the D-TCA model

Fig.4 shows the framework of the D-TCA model, which is divided into three parts, namely forward rules (FR), lane change (LC) decision, and unsuccessful LC. The updating rules of these parts are determined by LSTM (LSTM-FR), SVM (SVM-LD), and SVM (SVM-UL) networks, respectively. The data used for training these networks is the Next Generation Simulation (NGSIM) project dataset (i.e. the US Highway 101 Dataset), which records the real-time information (including speeds, acceleration, headway, etc) of vehicles passing through a certain section on the highway for a total of 45 minutes. This dataset has been widely adopted in recent years for traffic flow research ().

2.3.1. LSTM-FR network

LSTM is a time cyclic neural network, first proposed by Sepp Hochreiter and Jurgen Schmidhuber [64]. The network structure of LSTM-FR is designed into three layers, including an input layer, an output layer, and a hidden layer (see Fig.5). The input layer receives traffic state information of the subject vehicle () and of its surrounding vehicles, while the output layer exports the predicted acceleration of . Moreover, the hidden layer connects the previous two layers through a directed cycle,

forming an internal structure of the network [12]

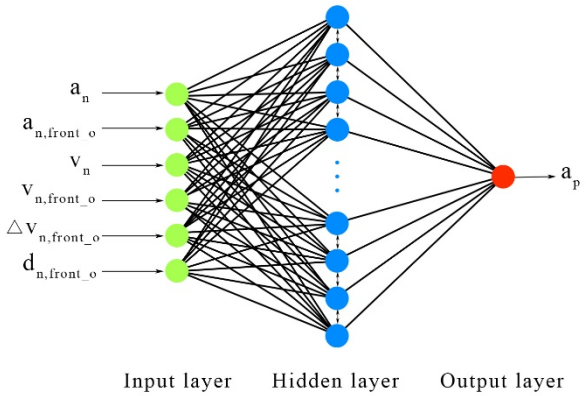

Fig.5 Network structure of LSTM

Drivers' behavior is affected by many factors, and the behavior of the previous moments may affect the driving decision on the current situation. LSTM-FR is used to mine the driving behavior characteristics (i.e. acceleration) based on historical data. The variables of the network are shown in Table 1.

Table 1 Input and output of the LSTM-FR network

Variables
Input
Output

Data preparation

From the original NGSIM dataset, the following data was deleted:

(1) the data of cars on lane 1, 5, 6, 7 and 8;

(2) the data of cars without preceding cars;

(3) the data of any vehicles other than cars (i.e. the non-car data, with the vehicle type being identified as type 1 and type 3);

(4) the data of lane changing cars if these cars have preceding cars that also perform lane changing operations;

Step (1) and (4) aim to minimize the impact of lane changing on car following behavior, Step (2) ensures normal car following behavior, and Step (3) extracts data only from cars. After the removal of the above data, 936 car following samples were retained. In order to reduce the influence of magnitude difference on the model, we use the MinMaxScaler method to standardize each variable into the range according to Eq.(2).

(2)

where is the standardized value, while and are the minimum and maximum values of the corresponding variable.

Training and testing

In deriving the network model, two thirds of the previously-obtained samples (624) were used for training, while the remaining ones (312) for testing. The number of neurons on each layer of LSTM-FR was specified as follows: 6 neurons on the first layer corresponding to the 6 input variables (in Table 1), 50 neurons on the hidden layer, and 1 neuron on the output layer representing the predicted acceleration. Meanwhile, the length of each time step was set as 10s, and the loss function "MAE" in Eq.(3) was adopted.

(3)

Where is the number of samples, while and are the output by the network and the actual acceleration value, respectively. The objective of the network training is to make MAE as small as possible. For the final (derived) model, the minimum value of MAE for the training and testing data reached 0.001 and 0.006, respectively.

2.3.2. SVM-LD network

SVM is a kind of generalized linear classifier that separates data in a binary way based on supervised learning, and was originally developed by Corinna Cortes and Vladimir Vapnik [65]. The network structure of SVM-LD is composed of three parts: an input, a hidden, and an output layers (See Fig.6). The input variables (on the input layer) first undergo nonlinear transformation, and are then classified according to support vectors in the feature space (on the hidden layer), and finally converted into the results (i.e. 1 or 0) (on the output layer).

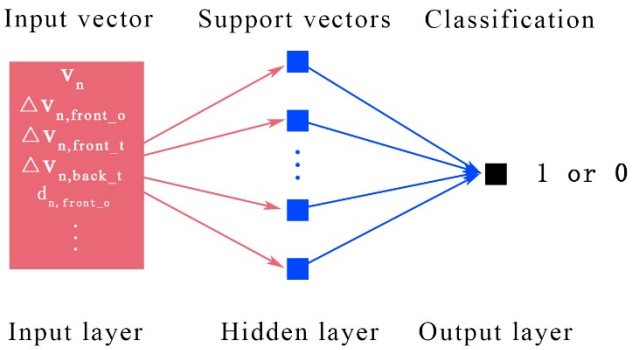

Fig.6 Network structure of SVM

Like car following, there exist many elements (such as headway, velocity, etc) that drivers consider when deciding whether or not to change lanes. SVM-LD is used to predict lane changing behavior of vehicles under certain driving conditions. The variables of the network are shown in Table 2. The output has two values: if output =1, the vehicle will change lanes; otherwise, if output = 0, the vehicle will remain in the current lane.

Table 2 Input and output of the SVM-LD network

	Variables
Input	

Output	0 or 1

Data preparation

The data used for training SVM-LD consists of two parts, namely, data of lane changing cars and data of car following cars. For lane changing cars, the values of the input variables (in Table 2) were extracted at the start time of the lane changing; while for car following cars, the values were obtained at all the time steps of the car following process.

From the NGSIM dataset, the following data was deleted:

(1) the same data as that depicted in Step (1), (2), and (3) in the data preparation for LSTM-FR;

(2) the data of cars that do not change lanes, cars whose both preceding and succeeding cars simultaneously change lanes, and cars that change lanes multiple times.

The retained data further underwent data standardization by means of the MinMaxScaler method. Finally, 863 samples were obtained, composed of 259 for lane changing and the remaining 604 for car following.

Training and testing

In calibrating the model, 70% (604) of the data was used for training, and the rest 30% (259) for testing. The classifier SVC in the sklearn.svm package was utilized, with the ‘linear’ kernel function being selected. The training accuracy of the SVM classifier was close to 1; but the testing accuracy varied, mainly depending on the parameter of "random number seed". We examined the testing accuracy under various values of this parameter, and obtained the highest accuracy at the value of 50. The prediction accuracy of the final classifier for both training and testing data was higher than 0.99.

2.3.3. SVM-UL network

In reality, the lane changing vehicle may return to the original lane when the driving condition of the original lane is better than that of the target lane. To model the unsuccessful lane changing behavior, SVM-UL is used to predict lane changing abandon decision. The variables of the network are presented in Table 3. The output has two outcomes: if output=1, the vehicle will return to the original lane (abandon decision being taken); otherwise, if output=0, the vehicle will maintain the lane changing maneuver (not abandoning).

Table 3 Input and output of the SVM-UL network

Variables
Input

,

Output 0 or 1

Data preparation

The dataset used for training SVM-UL originated from the previously obtained lane changing data for SVM-LD (described in Section 2.3.3), which was composed of 163 samples for successful lane changing and 30 for unsuccessful changing.

Training and testing

From the above dataset, 70% was randomly selected for training, and the remaining 30% for testing. The same SVM classifier and 'linear' kernel function used for deriving SVM-LD were applied, and the "random number seed" was set as 20 (after a number of trying). The prediction accuracy of the resultant SVM-UL classifier for both training and testing data was 0.879.

It was noted that the number of unsuccessful lane changing samples for inferring SVM-UL is smaller than would be required. Nevertheless, the obtained prediction accuracy demonstrates the potential and effectiveness of the proposed model. With a larger dataset, the data would become more capable of representing both successful and unsuccessful lane changing behavior. It is thus believed that the SVM-UL network would bring a greater improvement to the current experimental results.

2.3.4 Update rules

2.3.4.1. Forward rules

In the D-TCA model, contrasting with traditional CA updating rules, the cell moves forward according to the following steps,

Step1: acceleration: ;

Step2: position updating: +.

Where is the acceleration predicted by LSTM-FR based on the current input; *longitudinal length* denotes the longitudinal length of the cell; , , and refer to as the acceleration, position, and velocity of while as the maximum acceleration capacity of vehicles (see Section 2.2). Moreover, represents the space gap between and its preceding vehicle (i.e.) when is in State 0, 1, 3, or 4. In case that is in State 2, it is assumed that the vehicle occupies two lanes (including the original and target lanes), such that the vehicle does not only prohibit the overtaking behavior of its succeeding vehicles in the two lanes, but it is also blocked by its preceding vehicles in these lanes. To reflect the impact of this process on traffic flow, for State 2 is computed as follows.

(4)

The definition of and are described in Section 2.2.

According to Step1, is equal to the minimum value among the corresponding three variables. This does not only take into account the actual mechanical performance limitation of the vehicle, but also makes certain that the vehicle will not hit its preceding vehicle. In addition, ensures that the acceleration of the vehicle is an integer.

2.3.4.2. Lane changing rules

LC decision

Lane changing decision is predicted by SVM-LD, with the results indicating that will change lanes (if output =1) or remain in the current lane (if output = 0), respectively (see Section 2.3.2).

LC abandon

In practice, vehicles may return to the original lane in the process of lane changing, due to certain factors, such as the state of the lane changing vehicle and of its surrounding vehicles (which are taken as the input variables of SVM-UL (see Section 2.3.3). Lane changing abandon decision is forecasted by SVM-UL with two outcomes; will return to the original lane (abandon decision being taken) (if output =1) or maintain the lane changing maneuver (not abandoning) (if output = 0)

LC complete

When reaches the center of the target lane, the lane changing process is finished, and the vehicle is in State 4.

It should be noted that the forward rules are applied to each vehicle, while the LC decision rules are to vehicles that are in the process of moving forward, and the LC abandon and complete rules are to vehicles that are in the process of changing lanes.

3. Simulations and discussions

Numerical simulations for both the R-TCA and D-TCA models as well as for the TCA-H model proposed in the study [62] were carried out under periodic boundary conditions between different traffic density regions. In the simulation process of D-TCA, it is necessary to randomly give an initial state of the vehicle, such as the position and speed. And in the first quarter of the time step, we use R-TCA rules to update vehicles. The longitudinal and lateral length of each cell was set as 0.1m and 0.25m, respectively, and the length of each car was as 5m, spaning a total of 50 cells. The other parameters were specified as follows: the road length cells (5km), cell/s (129.6km/h), cell/s^{-2}, and cells according to the study [34].

3.1. Simulation performance

In order to examine the performance of D-TCA, we compared the simulation results by the model with the observed data from the NGSIM dataset. Fig.7 describes the observed and predicted acceleration of each vehicle among a fleet of 4 vehicles, with (vehicle) ID=2037, 2008, 2001, and 1998, respectively. Good matches between the two acceleration values at each time step for each of the vehicles can be seen, indicating of high accuracy of the model in predicting acceleration. In addition, we also inspected the simulated lane changing results of the vehicle (ID=64) against the real lane changing process under the same traffic conditions, as presented in Fig.8. Consistency between the observed and simulated lane numbers is demonstrated, signaling good performance of the model in re-generating the lane changing process of vehicles in actual traffic conditions.

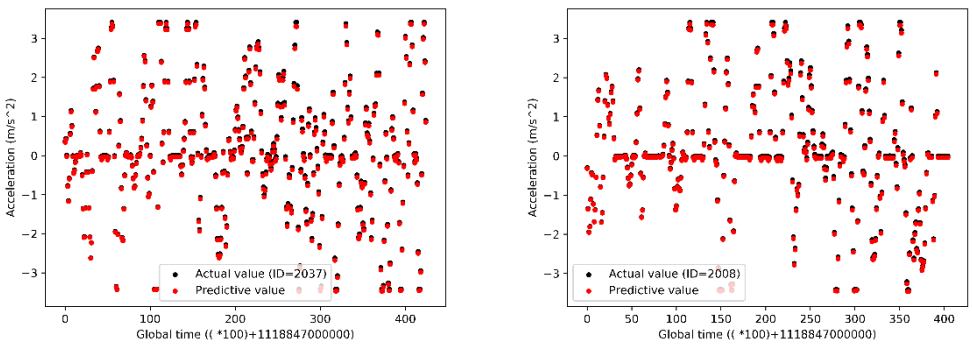

(a) (b)

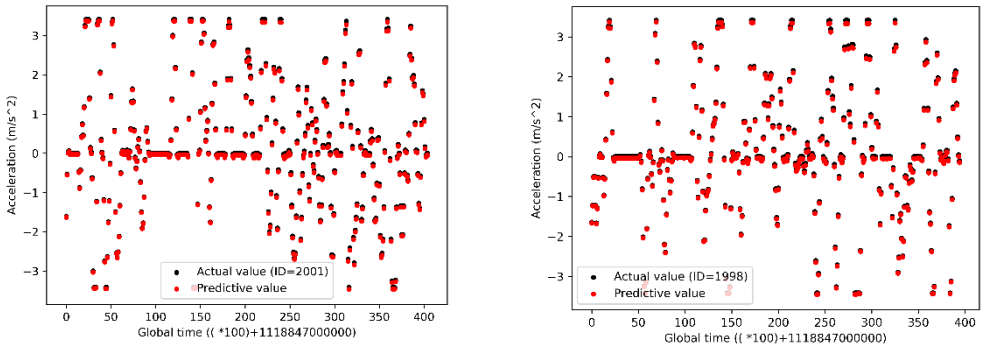

(c) (d)

Fig.7 Real acceleration and predicted acceleration of each vehicle for a fleet of 4 vehicles. ID = 2037 (a), 2008 (b), 2001 (c), and 1998 (d)

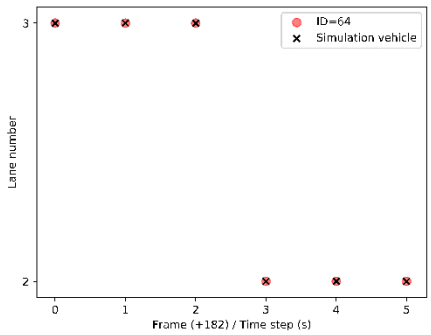

Fig.8 Schematic diagram of lane changing event

3.2. Fundamental diagram

The fundamental diagrams of R-TCA and D-TCA are visualized in Fig.9. It was noted that the flow of the former model is larger than that of the latter model, and a large gap exists between the two models in the middle- and high-density regions. Moreover, D-TCA can simulate the first-order phase transition from free flow to synchronized flow, which cannot be realized by R-TCA. The reason for this difference may lie in the random fluctuation of D-TCA during the updating process, which causes a sharp drop in traffic flow. The spatiotemporal diagram of D-TCA at density=0.2 is further described in Fig.10, showing that traffic congestion occurs under this density and spreads to the upstream.

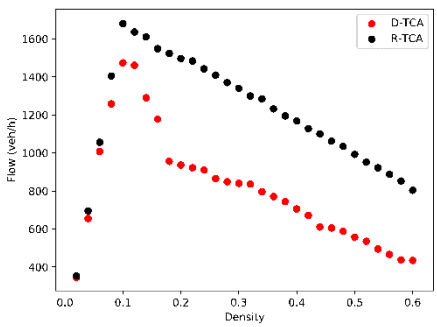

Fig.9 Fundamental diagrams of the R-TCA and D-TCA models.

(a)

(b)

Fig.10 Spatiotemporal diagram of the D-TCA model at density=0.2. (a) Left lane; (b) Right lane

3.3. Lane changing frequency

In this subsection as well as in Section 3.4 and 3.5, the results simulated by TCA-H and D-TCA were compared. Fig.11 shows the lane changing frequency obtained by the two models at different densities. The lane changing frequency of TCA-H is significantly greater than that of D-TCA, and the gap between the models is particularly large in the middle-density region.

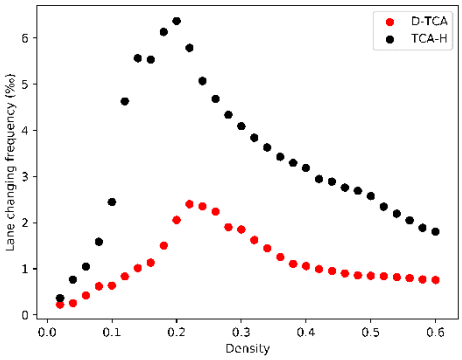

Fig.11 Lane changing frequency diagrams of the TCA-H and D-TCA models.

3.4. Lane changing duration

Fig. 12 depicts the average lane changing time obtained by the models at various densities. In the free flow area, the average lane changing time of the models is almost the same. However, as the density increases, deviation starts to appear and gradually becomes large, and reaches the peak at the highest density (density=0.6).

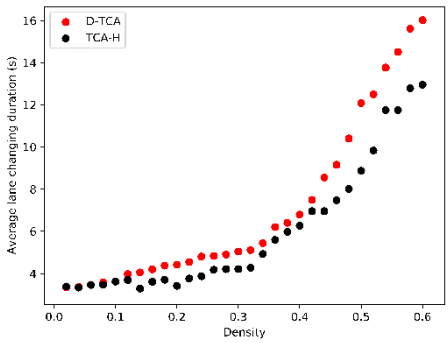

Fig.12 Average lane changing durations of the TCA-H and D-TCA models.

Moreover, we extracted the lane changing trajectory of the vehicle (ID=1778) from the NGSIM dataset and that of the corresponding vehicle simulated by D-TCA at density=0.2 (see Fig.13). It was observed that the lane changing trajectories of the two vehicles are similar, and that the speeds of these vehicles after lane changing are higher than those before the operation. Those results verify the effectiveness of the D-TCA model.

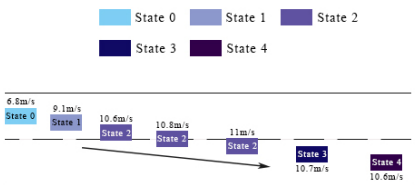

(a)

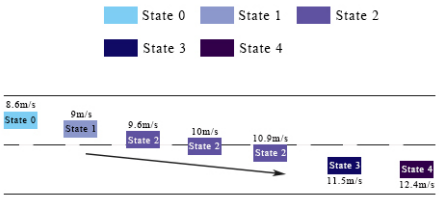

(b)

Fig.13 The lane changing trajectories of (a) the vehicle (ID=1778) from the NGSIM dataset and (b) a certain vehicle of the D-TCA model (density=0.2)

3.5. Unsuccessful lane changing frequency

Fig.14 visualizes the unsuccessful lane changing frequency of the models for the previously-illustrated two vehicles (i.e. the vehicle of ID=1778 and the corresponding simulated vehicle). There are almost no unsuccessful lane changing in the low-density area for both models. This can be attributed to the fact that vehicles can drive at higher speeds under free flow conditions, leading to smaller lane changing frequency and consequently smaller unsuccessful lane changing frequency. However, difference starts to emerge in the middle-and high-density regions. Regarding TCA-H, the unsuccessful lane changing frequency of the model increases sharply at the boundary between the low- and middle-density region as well as between the middle- and high-density area. In terms of D-TCA, the unsuccessful lane changing frequency is smaller than that of TCA-H in the middle-density region. However, when the density is higher than 0.3, this frequency increases considerably, much larger than that of TCA-H. This is consistent with the reality. Moreover, the comparison between Fig.12 and Fig.14 shows that the unsuccessful lane changing frequency and lane changing duration exhibit similar trends as the density goes up.

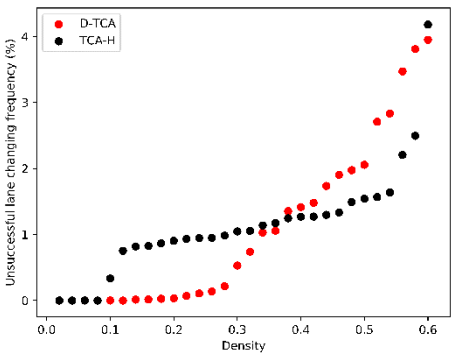

Fig.14 Unsuccessful lane changing frequency of the TCA-H and D-TCA models.

4. Conclusions

In this paper, we proposed a data-driven two-lane traffic flow model based on cellular automata. LSTM and SVM networks were applied to mine drivers' car following behavior, lane changing behavior, and unsuccessful lane changing behavior from real operation data of vehicles. According to actual driving characteristics, we improved the rules of moving forward and lane changing adopted in traditional CA models, and further designed new rules for unsuccessful lane changing.

Based on the proposed model, the following major results were obtained: (1) both the training and testing errors of the LSTM and SVM networks are relatively small, demonstrating good capacity of these models in mining real driving characteristics

from observed vehicle operation data; (2) the model can simulate the first-order phase transition from free flow to synchronized flow; (3) in the low-density region, the unsuccessful lane changing behavior barely occurs. However, when the density is higher than 0.3, the frequency of unsuccessful lane changing increases remarkably; (4) the higher the density, the higher the probability of unsuccessful lane changing and the longer the duration of successful lane changing.

Certain limitations exist regarding the proposed model. Firstly, in order to simplify the modelling process, the lane changing angle () was assumed to be a fixed value. Nevertheless, in actual lane changing processes, is not constant, making the above assumption not realistic. Secondly, due to the limited number of unsuccessful lane changing samples, the accuracy of the SVM-UL classifier is not high. Nevertheless, as stated in Section 2.3.3, SVM-UL introduces more practical updating rules for unsuccessful lane changing, and we believe that the network parameters would be better calibrated if the amount of data is larger and that the model would bring a greater improvement over the current results.

Acknowledgements

This work was supported by National Key R&D Program of China (No. 2018YFB1600900); the National Natural Science Foundation of China (No. 71621001, 71631002, 71771021); the Fundamental Research Funds for the Central Universities (No. 2020YJS078).

References

[1] M.J. Lighthill, G.B. Whitham, On kinematic waves. ii. A theory of traffic flow on long crowded roads, Proc. R. Soc. Lond. Ser. A Math. Phys. Eng. Sci., 1955, 229(1178): 317-345.

[2] P.I. Richards, Shock waves on the highway, Operations research, 1956, 4(1): 42-51.

[3] I. Prigogine, R. Herman, Kinetic theory of vehicular traffic, New York: American Elsevier, 1971, DOI.

[4] S.L. Paveri-Fontana, On boltzmann-like treatments for traffic flow. a critical review of the basic model and an alternative proposal for dilute traffic analysis, Transportation Research, 1975, 9: 225-235.

[5] T. M., H. A., H. D., Derivation, properties, and simulation of a gas-kinetic-based, nonlocal traffic model, Phys. Rev. E, 1999, 59(1): 239-253.

[6] R. A, Vehicle Movements in a platoon, Oesterreichisches Ingenieur-Archir, 1950, 4: 193-215.

[7] L.A. Pipes, An Operational Analysis of Traffic Dynamics, Journal of Appied Physics, 1953, 24(3): 274-281.

[8] M. Cremer, J. Ludwig, A fast simulation model for traffic flow on the basis of Boolean operations, Mathematics of cellular automata. Reviews of Modern Physics, 1983, 55: 601-644.

[9] Y. Dou, F. Yan, D. Feng, Lane changing prediction at highway lane drops using support vector machine and artificial neural network classifiers, 2016 IEEE International Conference on Advanced Intelligent Mechatronics (AIM), 2016, DOI.

[10] X. Huang, J. Sun, J. Sun, A car-following model considering asymmetric driving behavior based on long short-term memory neural networks, Transportation Research Part C: Emerging Technologies, 2018, 95: 346-362.

[11] Z. Zhao, W. Chen, X. Wu, P.C.Y. Chen, J. Liu, LSTM network: a deep learning approach for short-term traffic forecast, IET Intelligent Transport Systems, 2017, 11: 68-75.

[12] D.-F. Xie, Z.-Z. Fang, B. Jia, Z. He, A data-driven lane-changing model based on deep learning, Transportation Research Part C: Emerging Technologies, 2019, 106: 41-60.

[13] S. Panwai, H. Dia, Neural Agent Car-Following Models, IEEE Transactions on Intelligent Transportation Systems, 2007, 8(1): 60-70.

[14] A. Khodayari, A. Ghaffari, R. Kazemi, R. Braunstingl, A Modified Car-Following Model Based on a Neural Network Model of the Human Driver Effects, IEEE Transactions on Systems, Man, and Cybernetics - Part A: Systems and Humans, 2012, 42(6): 1440-1449.

[15] C. Ding, W. Wang, X. Wang, M. Baumann, A Neural Network Model for Driver's Lane-Changing Trajectory Prediction in Urban Traffic Flow, Mathematical Problems in Engineering, 2013, 2013: 1-8.

[16] J. Zheng, K. Suzuki, M. Fujita, Car-following behavior with instantaneous driver–vehicle reaction delay: A neural-network-based methodology, Transportation Research Part C: Emerging Technologies, 2013, 36: 339-351.

[17] Z. He, L. Zheng, W. Guan, A simple nonparametric car-following model driven by field data, Transportation Research Part B: Methodological, 2015, 80: 185-201.

[18] Y. Dou, F. Yan, D. Feng, Lane changing prediction at highway lane drops using support vector machine and artificial neural network classifiers, IEEE International Conference on Advanced Intelligent Mechatronics, 2016, DOI.

[19] M. Zhou, X. Qu, X. Li, A recurrent neural network based microscopic car following model to predict traffic oscillation, Transportation Research Part C: Emerging Technologies, 2017, 84: 245-264.

[20] X. Wang, R. Jiang, L. Li, Y. Lin, X. Zheng, F.-Y. Wang, Capturing Car-Following Behaviors by Deep Learning, IEEE Transactions on Intelligent Transportation Systems, 2018, 19(3): 910-920.

[21] Y. Wang, D. Zhang, Y. Liu, B. Dai, L.H. Lee, Enhancing transportation systems via deep learning: A survey, Transportation Research Part C: Emerging Technologies, 2019, 99: 144-163.

[22] M. Zhu, Y. Wang, Z. Pu, J. Hu, X. Wang, R. Ke, Safe, efficient, and comfortable velocity control based on reinforcement learning for autonomous driving, Transportation Research Part C: Emerging Technologies, 2020, 117.
[23] J. Tanimoto, Evolutionary Games with Sociophysics Analysis of Traffic Flow and Epidemics, Springer, 2019, DOI.
[24] R. Barlovic, L. Santen, A.Schadschneider, M. Schreckenberg, Metastable states in cellular automata for traffic flow, Eur. Phys. J. B, 1998, 5: 793-800.
[25] M. Takayasu, H. Takayasu, 1/f noise in a traffic model, Fractals, 1993, 1: 860-866.
[26] M.E. Lárraga, L. Alvarez-Icaza, Cellular automaton model for traffic flow based on safe driving policies and human reactions, Physica A: Statistical Mechanics and its Applications, 2010, 389(23): 5425-5438.
[27] J.-f. Tian, N. Jia, N. Zhu, B. Jia, Z.-z. Yuan, Brake light cellular automaton model with advanced randomization for traffic breakdown, Transportation Research Part C: Emerging Technologies, 2014, 44: 282-298.
[28] B.S. Kerner, S.L. Klenov, D.E. Wolf, Cellular automata approach to three-phase traffic theory, Journal of Physics A: Mathematical and General, 2002, 35: 9971-10013.
[29] Y.-S. Qian, X. Feng, J.-W. Zeng, A cellular automata traffic flow model for three-phase theory, Physica A: Statistical Mechanics and its Applications, 2017, 479: 509-526.
[30] K. Nagel, M. Schreckenberg, A cellular automata model for traffic flow, J. Phys. I France, 1992, 2.
[31] E. Brockfeld, R. Barlovic, A. Schadschneider, M. Schreckenberg, Optimizing traffic lights in a cellular automaton model for city traffic, Phys. Rev. E, 2001, 64: 056132.
[32] G.H. Bham, R.F. Benekohal, A high fidelity traffic simulation model based on cellular automata and car-following concepts, Transportation Research Part C: Emerging Technologies, 2004, 12(1): 1-32.
[33] S.F. Hafstein, R. Chrobok, A. Pottmeier, M. Schreckenberg, F.C. Mazur, A high-resolution cellular automata traffic simulation model with application in a freeway traffic information system, Computer-Aided Civil and Infrastructure Engineering, 2004, 19: 338-350.
[34] L.W. Lan, Y.-C. Chiou, Z.-S. Lin, C.-C. Hsu, A refined cellular automaton model to rectify impractical vehicular movement behavior, Physica A: Statistical Mechanics and its Applications, 2009, 388(18): 3917-3930.
[35] H.-Y. Shang, Y. Peng, A new three-step cellular automaton model considering a realistic driving decision, Journal of Statistical Mechanics: Theory and Experiment, 2012, 2012(10).
[36] B.S. Kerner, S.L. Klenov, G. Hermanns, M. Schreckenberg, Effect of driver over-acceleration on traffic breakdown in three-phase cellular automaton traffic flow models, Physica A: Statistical Mechanics and its Applications, 2013, 392(18): 4083-4105.
[37] T. Chmura, B. Herz, F. Knorr, T. Pitz, M. Schreckenberg, A Simple Cellular Automaton Model with Limited Braking Rule, Traffic and Granular Flow'13, Springer, 2015, DOI: 591-597.
[38] J. Tian, G. Li, M. Treiber, R. Jiang, N. Jia, S. Ma, Cellular automaton model simulating spatiotemporal patterns, phase transitions and concave growth pattern of oscillations in traffic flow, Transportation Research Part B: Methodological, 2016, 93: 560-575.
[39] H.A. Guzmán, M.E. Lárraga, L. Alvarez-Icaza, J. Carvajal, A cellular automata model for traffic flow based on kinetics theory, vehicles capabilities and driver reactions, Physica A: Statistical Mechanics and its Applications, 2018, 491: 528-548.
[40] X. Wang, Y. Xue, B.-l. Cen, P. Zhang, H.-d. He, Study on pollutant emissions of mixed traffic flow in cellular automaton, Physica A: Statistical Mechanics and its Applications, 2020, 537.
[41] J.-W. Zeng, Y.-S. Qian, S.-B. Yu, X.-T. Wei, Research on critical characteristics of highway traffic flow based on three phase traffic theory, Physica A: Statistical

Mechanics and its Applications, 2019, 530.
[42] J. Zeng, Y. Qian, Z. Lv, F. Yin, L. Zhu, Y. Zhang, D. Xu, Expressway traffic flow under the combined bottleneck of accident and on-ramp in framework of Kerner's three-phase traffic theory, Physica A: Statistical Mechanics and its Applications, 2021, 574.
[43] J. Zeng, Y. Qian, P. Mi, C. Zhang, F. Yin, L. Zhu, D. Xu, Freeway traffic flow cellular automata model based on mean velocity feedback, Physica A: Statistical Mechanics and its Applications, 2021, 562.
[44] J. Ji, L. Lu, Z. Jin, S. Wei, L. Ni, A cellular automata model for high-density crowd evacuation using triangle grids, Physica A: Statistical Mechanics and its Applications, 2018, 509: 1034-1045.
[45] X. Li, F. Guo, H. Kuang, Z. Geng, Y. Fan, An extended cost potential field cellular automaton model for pedestrian evacuation considering the restriction of visual field, Physica A: Statistical Mechanics and its Applications, 2019, 515: 47-56.
[46] L. Yang, J. Zheng, Y. Cheng, B. Ran, An asymmetric cellular automata model for heterogeneous traffic flow on freeways with a climbing lane, Physica A: Statistical Mechanics and its Applications, 2019, 535.
[47] X. Zhou, J. Hu, X. Ji, X. Xiao, Cellular automaton simulation of pedestrian flow considering vision and multi-velocity, Physica A: Statistical Mechanics and its Applications, 2019, 514: 982-992.
[48] D.-J. Fu, Q.-L. Li, R. Jiang, B.-H. Wang, A simple cellular automaton model with dual cruise-control limit in the framework of Kerner's three-phase traffic theory, Physica A: Statistical Mechanics and its Applications, 2020, 559.
[49] W. Hua, Y. Yue, Z. Wei, J. Chen, W. Wang, A cellular automata traffic flow model with spatial variation in the cell width, Physica A: Statistical Mechanics and its Applications, 2020, 556.
[50] M. Layegh, B. Mirbaha, A.A. Rassafi, Modeling the pedestrian behavior at conflicts with vehicles in multi-lane roundabouts (a cellular automata approach), Physica A: Statistical Mechanics and its Applications, 2020, 556.
[51] D. Miyagawa, G. Ichinose, Cellular automaton model with turning behavior in crowd evacuation, Physica A: Statistical Mechanics and its Applications, 2020, 549.
[52] E.N.M. Cirillo, F.R. Nardi, C. Spitoni, Phase transitions in random mixtures of elementary cellular automata, Physica A: Statistical Mechanics and its Applications, 2021, 573.
[53] Y. Huang, D. Li, J. Cheng, Simulation of pedestrian–vehicle interference in railway station drop-off area based on cellular automata, Physica A: Statistical Mechanics and its Applications, 2021, 579.
[54] D. Kong, L. Sun, J. Li, Y. Xu, Modeling cars and trucks in the heterogeneous traffic based on car–truck combination effect using cellular automata, Physica A: Statistical Mechanics and its Applications, 2021, 562.
[55] Y.-f. Qiao, Y. Xue, X. Wang, B.-l. Cen, Y. Wang, W. Pan, Y.-x. Zhang, Investigation of PM emissions in cellular automata model with slow-to-start effect, Physica A: Statistical Mechanics and its Applications, 2021, 574.
[56] R. Zhao, Y. Zhai, L. Qu, R. Wang, Y. Huang, Q. Dong, A continuous floor field cellular automata model with interaction area for crowd evacuation, Physica A: Statistical Mechanics and its Applications, 2021, 575.
[57] X.-G. Li, B. Jia, Z.-Y. Gao, R. Jiang, A realistic two-lane cellular automata traffic model considering aggressive lane-changing behavior of fast vehicle, Physica A: Statistical Mechanics and its Applications, 2006, 367: 479-486.
[58] S. Kukida, J. Tanimoto, A. Hagishima, Analysis of the Influence of Lane Changing on Traffic-Flow Dynamics Based on the Cellular Automaton Model, International Journal of Modern Physics C, 2011, 22(03): 271-281.
[59] J. Tanimoto, X. An, Improvement of traffic flux with introduction of a new lane-change protocol supported by Intelligent Traffic System, Chaos, Solitons & Fractals, 2019, 122: 1-5.
[60] J. Tanimoto, M. Futamata, M. Tanaka, Automated vehicle control systems need to solve social dilemmas to be disseminated, Chaos, Solitons & Fractals, 2020, 138.
[61] A. Schadschneider, M. Schreckenberg, Cellular automation models and traffic

flow, Journal of Physics A: Mathematical and General, 1993, 26(15): L679-L683.
[62] X.-C. Shang, X.-G. Li, D.-F. Xie, B. Jia, R. Jiang, Two-lane traffic flow model based on regular hexagonal cells with realistic lane changing behavior, Physica A: Statistical Mechanics and its Applications, 2020, 560.
[63] M.Rickert, K.Nagel, M.Schreckenberg, A.Latour, Two lane traffic simulations using cellular automata, Physica A: Statistical Mechanics and its Applications, 1996, 231.
[64] S. Hochreiter, J. Schmidhuber, Long Short-Term Memory, Neural Computation, 1997, 9: 1735-1780.
[65] C. Cortes, V. Vapnik, Support-vectorNetworks, Machine Leaming, 1995, 20: 273-297.